Journal of Applied Mechanics and Technical Physics, Vol. 48, No. 6, pp. 887–896, 2007

EFFECT OF THE GRAIN SIZE ON THE MACROSCOPIC RESPONSE OF ALUMINUM TO SHOCK LOADING

Yu. I. Meshcheryakov,[1] **A. K. Divakov,**[1]
N. I. Zhigacheva,[1] **and M. M. Myshlyaev**[2]

UDC 539.374

Shock tests of two lots of a 1420 *aluminum–lithium alloy are performed. The mean grain size is* 24 μm *in the first lot and* 1.6 μm *in the second lot obtained by the method of equal-channel angular pressing. Two characteristics of dynamic strength of the material were determined in experiments on the high-velocity impact of flat samples: threshold of dynamic stability with respect to compression on the fore front of the compression pulse and spall strength of the material. The materials of both types have an identical threshold of dynamic stability with respect to compression, whereas the spall strength of the microcrystalline alloy is* 20% *greater than the spall strength of the polycrystalline alloy. The reason is the consumption of energy on structure formation in the coarse-grain material in passing to a larger-scale structural level* (*in the case with a fine-grain material, such a structure is available in the initial state*). *The experiments reveal the presence of a second plastic front whose amplitude is approximately* 10% *of the first plastic front.*

Key words: *structural level, microcrystalline, high-velocity impact, spall strength, threshold of dynamic stability.*

Introduction. Owing to the recent development of mesomechanics (a new field of mechanics of deformable solids), experimental data were obtained and theoretical models were developed, which take into account the permanent exchange of momentum and energy between the mesolevel and macrolevel in the course of dynamic deformation [1–4]. These models predict that the possibilities of deformation at the lower (atomic-dislocation) structural level are exhausted at a certain threshold strain, and a transition occurs from this level to a larger-scale structural level, which was called the mesostructure. By now, the concept of the mesostructure (especially in a dynamically deformed solid) has been completely defined neither from the viewpoint of physics of elementary processes nor from the viewpoint of mechanics of deformable solids. As we consider only the processes of dynamic deformation in the present paper, we present the mesostructure as a spatial field structure with correlated motion of elementary strain carriers of a lower-scale level (comparable, for instance, with the dislocation level). In a dynamically deformed medium, the transition to a larger-scale structural level means that the entire deformation domain is divided into volumes that are independent strain carriers. At the same time, the motion of large-scale strain carriers can be rather nonuniform in the space of velocities, i.e., a significant scatter in velocities with respect to the mean mass velocity of the deformed medium may be observed. The scale of the new structural element (mesoparticle) may fail to coincide with the size characteristics of the original structure of the material, for example, with the grain size. Thus, the question arises: How does the transition of dynamic deformation from one level to another affect the macroscopic response of the material to shock loading, depending on the parameters of the original structure of the material?

[1]Institute of Problems of Mechanical Engineering, Russian Academy of Sciences, St. Petersburg 199178; yum@fracture.ipme.ru, ymesch@impact.ipme.ru. [2]Baikov Institute of Metallurgy and Material Science, Russian Academy of Sciences, Moscow 119991. Translated from Prikladnaya Mekhanika i Tekhnicheskaya Fizika, Vol. 48, No. 6, pp. 135–146, November–December, 2007. Original article submitted December 6, 2005; revision submitted December 5, 2006.

0021-8944/07/4806-0887

TABLE 1

Results of Shock Tests of a 1420 Aluminum Alloy with a Grain Size of 24 μm

Test number	U_{imp}, m/sec	h_{targ}, mm	h_{imp}, mm	U_C, m/sec	U_D, m/sec	$U_{fs}^{\max}$, m/sec	U_{pl2}, m/sec	C_{pl1}, m/sec	C_{pl2}, m/sec	ΔW, m/sec
1	97.2	4.47	1.96	85.6	82.3	88.0	1.1	—	—	—
2	139.1	4.41	1.93	127.9	125.3	130.7	3.4	5.26	4.02	122.9
3	212.5	4.43	1.92	202.7	184.2	210.7	8.0	5.23	4.10	126.5
4	310.0	4.42	1.98	288.8	267.0	296.5	7.7	5.29	4.33	124.0

TABLE 2

Results of Shock Tests of a 1420 Aluminum Alloy with a Grain Size of 1.6 μm

Test number	U_{imp}, m/sec	h_{targ}, mm	h_{imp}, mm	U_C, m/sec	U_D, m/sec	$U_{fs}^{\max}$, m/sec	U_{pl2}, m/sec	C_{pl1}, m/sec	C_{pl2}, m/sec	ΔW, m/sec
1	98.7	4.29	1.89	85.6	82.3	99.0	1.1	—	—	—
2	136.2	4.28	1.89	127.9	125.3	136.3	3.4	5.26	4.02	—
3	200.0	4.30	1.90	202.7	184.2	200.5	8.0	5.23	4.10	146.3
4	280.3	4.30	1.91	288.8	267.0	279.0	7.7	5.29	4.33	146.3

To answer this question, we performed a comparative experimental study of the shock-wave behavior of a 1420 polycrystalline aluminum–lithium alloy with different grain sizes in the original structure:

1) coarse-grain material (with a mean grain size $\delta = 24$ μm);

2) fine-grain material (with a mean grain size $\delta = 1.6$ μm).

The second material was obtained by equal-channel angular pressing of the first material [5].

1. Experimental Technique and Results. The shock tests under uniaxial strain conditions in the range of impact velocities of 80–300 m/sec were performed in a single-stage light-gas gun with a caliber of 37 mm. In all experiments, the impact velocity was chosen such that the spall on the back side of flat targets was obtained. For structural changes initiated by shock loading to be preserved, the targets of the examined material, 20 mm in diameter and 4 mm thick, were conically inserted into disks made of a D-16 alloy, 52 mm in diameter and 4 mm thick. This procedure prevented repeated passage through the sample of the waves reflected from the side surfaces of the targets. Impactors approximately 2 mm thick were made of the D-16 aluminum alloy whose acoustic impedance is close to the acoustic impedance of the 1420 alloy, which ensures impact symmetry.

The velocity profiles of the free surface of the targets were measured by a two-channel velocity interferometer with a high resolution in space ($\approx$50 μm) and time ($\approx$1 nsec). In addition, the technique used allows one to measure the root-mean-square deviations of particle velocity (square root from the dispersion) owing to local shear processes in a dynamically deformed material at the mesoscopic scale [6].

The test results for both materials are summarized in Tables 1 and 2 (U_{imp} is the impact velocity, h_{targ} is the target thickness, h_{imp} is the impactor thickness, U_C and U_D are the velocities on the free surface on the fore front at the beginning and end of the structural transition, $U_{fs}^{\max}$ is the maximum velocity of the free surface of the target, U_{pl2} is the velocity of the free surface corresponding to the second plastic front, C_{pl1} and C_{pl2} are the velocities of the first and second plastic fronts, respectively, and $\Delta W = W_{\max} - W_{\min}$ is the difference in velocities on the rear front of the compression pulse due to spall fracture). Figure 1 shows the velocity of the free surface versus time $U_{fs}(t)$ for the 1420 alloy. The amplitude of the elastic precursor in both materials is almost identical, though the elastic precursor in the first material is followed by a valley caused by relaxation.

The changes in the mean mass velocity on the plastic front of the compression pulse $U_{fs}(t)$ and in the mass velocity dispersion $D(t)$ at the mesolevel turned out to be interrelated. For materials of both types, the mean velocity drastically increases until the velocity dispersion vanishes (see below). The point C on the profile corresponds to a decrease in the velocity dispersion to zero. After this moment, the plastic front becomes less steep (segment CD) The segments BC of the plastic front where the velocity drastically increases are parallel for both materials, though

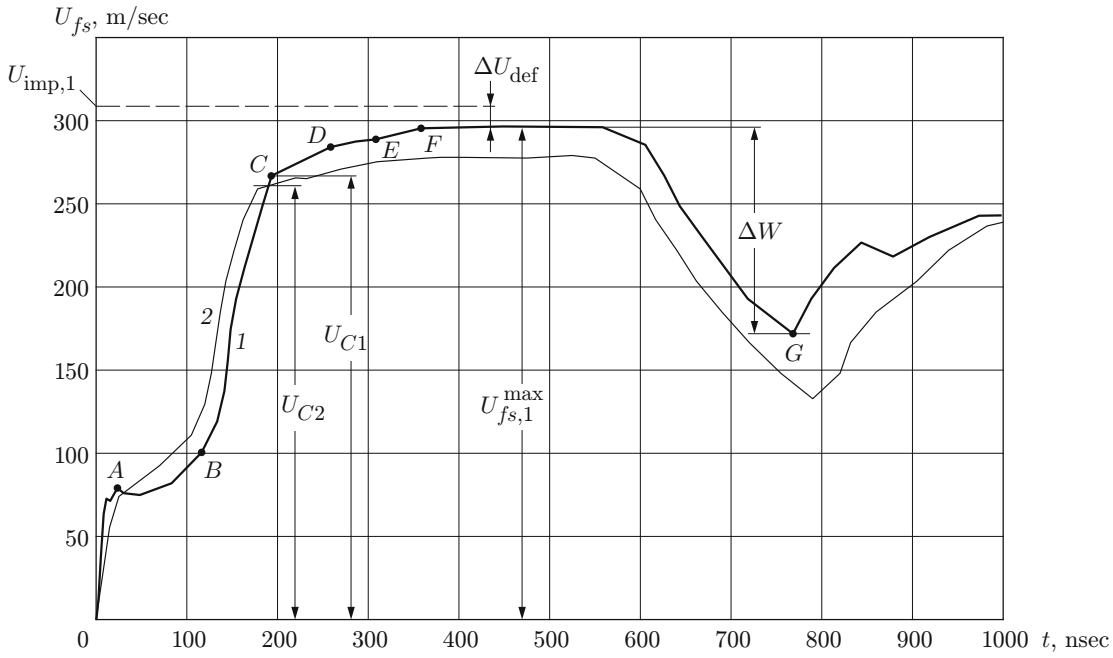

Fig. 1. Velocity of the free surface versus time: 1) $\delta = 24$ μm and $U_{\text{imp}} = 310$ m/sec; 2) $\delta = 1.6$ μm and $U_{\text{imp}} = 280.3$ m/sec.

the velocity of plastic front propagation in the fine-grain material is somewhat greater than that in the coarse-grain material (see Sec. 3). The difference occurs after a small (≈22 nsec) horizontal plateau (segment DE). For the alloy of the second type, the velocity of the free surface on the segment EF gradually approaches the value equal to the impact velocity in a symmetric collision, whereas the dependence $U_{fs}(t)$ for the alloy of the first type contains a mass velocity defect ΔU_{def} determined by the difference between the impact velocity in a symmetric collision and the velocity of the free surface on the compression pulse plateau obtained in independent measurements by an interferometer:

$$\Delta U_{\text{def}} = U_{\text{imp}} - U_{fs}^{\max}.$$

The examined materials were found to have different defects of mass velocity. For the fine-grain material, $\Delta U_{\text{def}} = 0$ in the entire range of impact velocities, i.e., the criterion of doubling of the mass velocity U_p on the free surface of a flat target is satisfied: $2U_p = U_{fs}^{\max} = U_{\text{imp}}$. For the coarse-grain material, the defect is 5–10% of the maximum value of the free surface velocity. Possible reasons for the different behavior of the two materials are discussed in Sec. 3.

In addition to the mass velocity defect determining the loss of momentum and energy under shock compression, another parameter measured in the experiments was the spall strength. The value of the spall strength σ for the materials of both types was determined from the formula for the free surface velocity as a function of time

$$\sigma = 0.5\rho_0 C_0(\Delta W + \delta W), \tag{1}$$

where C_0 is the volume velocity of sound and δW is the correction that takes into account the difference in velocities of the incident pulse on the unloading segment and the front of the spall pulse reflected from the spall surface [7]. The value of this correction is estimated by the formula

$$\delta W = \Big(\frac{h}{C_0} - \frac{h}{C_l}\Big)\frac{|W_1 W_2|}{|W_1| + W_2}, \tag{2}$$

where $h = C_l \Delta t/2$ is the thickness of the spall plate, C_l is the longitudinal velocity of sound, Δt is period of the change in velocity in the spall plate, and W_1 and W_2 are the accelerations of the free surface in the incident unloading wave and in the front of the spall pulse, respectively. The results of processing of the free surface velocity profiles for both materials and the spall strengths calculated by formulas (1) and (2) are listed in Tables 3 and 4. Figure 2

TABLE 3

Spall Strength of the 1420 Aluminum Alloy with a Grain Size of 24 μm

Calculation variant	U_{imp}, m/sec	ΔW, m/sec	δW, m/sec	C_l, 10^5 cm/sec	C_0, 10^5 cm/sec	σ, GPa
1	139.1	122.9	3.57	6.385	5.333	0.913
2	212.5	126.5	10.20	6.385	5.333	0.966
3	310.0	124.0	20.00	6.385	5.333	1.040

TABLE 4

Spall Strength of the 1420 Aluminum Alloy with a Grain Size of 1.6 μm

Calculation variant	U_{imp}, m/sec	ΔW, m/sec	δW, m/sec	C_l, 10^5 cm/sec	C_0, 10^5 cm/sec	σ, GPa
1	200.0	146.3	4.86	6.34	5.333	1.090
2	280.3	146.3	12.90	6.34	5.333	1.146

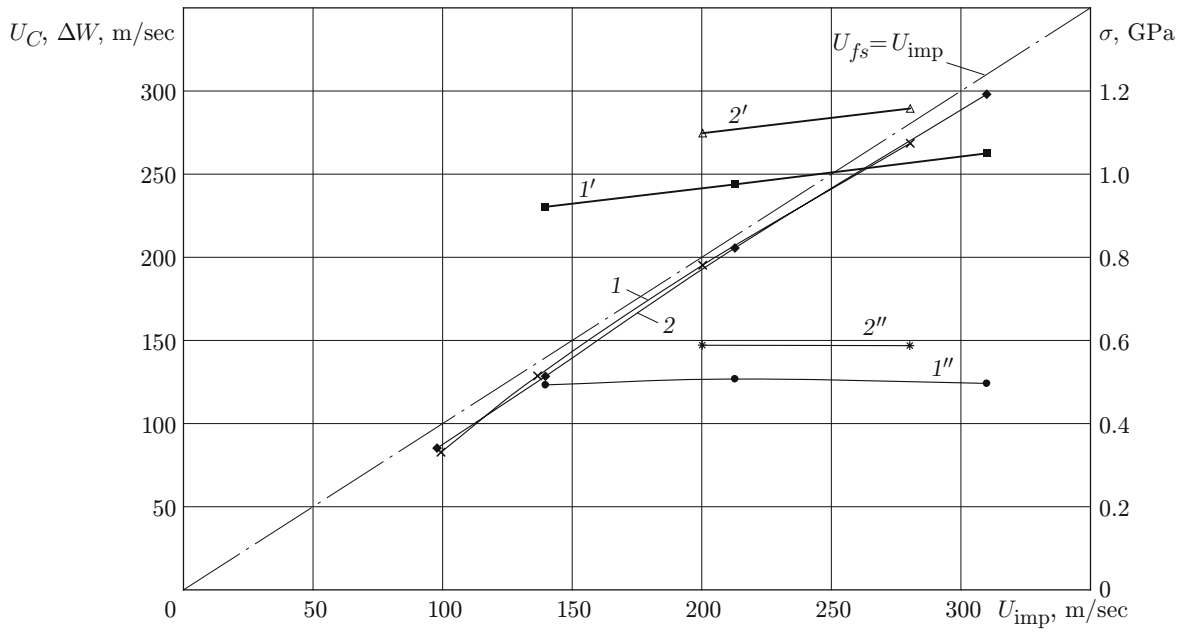

Fig. 2. Threshold velocity of the structural transition U_C (1 and 2), spall strength σ (1′ and 2′), and ΔW (1″ and 2″) versus the impact velocity: $\delta = 1.6$ (1, 1′, and 1″) and 24 μm (2, 2′, and 2″).

shows the spall velocity and the threshold velocity of the structural transition as functions of the impact velocity. The spall strength of the fine-grain alloy is seen to be almost 20% higher than the spall strength of the original (coarse-grain) alloy. Moreover, for the material with a grain size $\delta = 1.6$ μm, the spall occurs at a significantly greater impact velocity (200 m/sec) that for the material with a grain size $\delta = 24$ μm ($U_{\text{imp}} = 139.1$ m/sec). For comparison, Fig. 2 also shows the dependence $\Delta W(U_{\text{imp}})$. In contrast to the curves $\sigma(U_{\text{imp}})$, the curves $\Delta W(U_{\text{imp}})$ are parallel to the abscissa axis. The use of correction (2) increases the spall strength with increasing strain rate for both materials.

2. Discussion. A drastic change in the slope of the plastic front under uniaxial strain conditions was first encountered in tests of a 6061-T-6 aluminum alloy [8]. Without analyzing the physics of the phenomenon, Barker et al. [8] attributed this effect to the influence of the strain rate on the mechanical properties of the material.

The difficulty in identification of the structural transition examined is the fact that the changes in the form and structure of the plastic front are affected by interaction between the elastic precursor reflected from the free surface of the target and the plastic front, which was first noted in [9]. The issue of interaction of the elastic

precursor with the incoming plastic front is currently under discussion. The analysis performed in [10] showed that this interaction alters the slope of the upper part of the plastic front. In addition, the maximum value of mass velocity on the compression pulse plateau is reduced. Numerical results are also presented in [11], where both the elastic precursor and the plastic front are assumed to have an identical wave nature, i.e., propagation of both fronts is described by equations of the hyperbolic type. In reality, propagation of the elastic precursor obeys a hyperbolic equation, while the plastic front has a relaxation nature, and its propagation is determined by the transport laws described by a parabolic equation or by a mixed-type equation [12, 13]. Because of the difference in the physical nature of the elastic and plastic fronts, their interaction turns out to be insignificant. As a result, they intersect almost without any changes in amplitude (only a small perturbation on the plastic front is observed) [14]. As a whole, in the case of multiple interactions between the elastic precursor and the plastic front, the effect of this interaction is rather small, because, first, the change in material density on the plastic front is only fractions of a percent, so that it does not provide stiff reflection of the elastic wave, and, second, in the case of alternating reflections of the elastic precursor from the plastic front and from the free surface of the target, the character of its interaction with these surfaces is different: after interaction with the free surface, the sign of mass velocity in the reflected elastic wave changes to the opposite one, while the sign remains unchanged in interaction with the plastic front. Thus, the amplitude of the plastic front decreases in the first interaction with the elastic precursor, increases in the second interaction, etc. As a result, interaction of the elastic precursor with the plastic front does not affect the maximum value of mass velocity on the compression pulse plateau.

As applied to the experiments described here, the following fact should be taken into account: the amplitude of the elastic precursor in all experiments was almost identical, but a decrease in the maximum value of mass velocity on the compression pulse plateau was observed only for the material of the first type. For the material of the second type, this value was equal to the impact velocity in a symmetric collision, which evidences that the rule of doubling of mass velocity on the free surface of the target is satisfied. The information given above allows us to assume that a drastic change in the slope of the plastic front is caused by a change in the material structure at a certain threshold value of mass velocity on the plastic front U_C (point C in Fig. 1). The threshold velocity of the structural transition U_C turned out to be identical for materials of both types for one impact velocity. It is also worth noting that, though the threshold velocity of the structural transition linearly increases with increasing impact velocity, the duration of the compression pulse front before the beginning of this transition is identical for all loading velocities and coincides with the period of nonzero dispersion of mass velocity. Figure 3 shows the velocity profiles for the free surface of the material with a grain size $\delta = 1.6$ μm obtained for different impact velocities. Though the threshold velocities of the beginning of the structural transition U_{C1}, U_{C2}, and U_{C3} were different in the experiments, the duration of the plastic front and the period with nonzero dispersion are approximately identical ($\approx$140 nsec). In relaxation models of uniaxial deformation, the plastic front is the front of stress relaxation [15], and its duration is determined by the stress relaxation time. The processes of dynamic deformation on the plastic front were previously thought to be caused by generation and motion of dislocations. Detailed studies performed in 1970s–1980s, however, showed that it is insufficient to analyze dynamic deformation with the use of dislocation mechanisms only. For the dynamic response of the material to shock loading to be adequately described, it is necessary to consider a larger-scale level of deformation, namely, the so-called mesolevel. In the course of material deformation, mesostructures are formed in the nonlinear region of elastic deformation. It has been proved theoretically that mesostructures emerge under the action of pressure and shear [16]. Large-scale structures appear long before the transition to macroscopic plasticity. In the case of quasi-static deformation, these structures may disappear when external pressure is removed, if the strain gradient does not exceed a critical value at which a bifurcation transition occurs, leading to formation of irreversible mesostructures. It is known that uniaxial deformation in plane shock waves also occurs under the action of hydrostatic pressure and shear. Because of this fact, conditions during the action of the compression pulse are the same as those that may initiate generation of large-scale structure.

The mass velocity dispersion in the compression wave, which was recorded in shock experiments [6], is caused by fluctuations of large-scale structures (granular temperature). The time during which the dispersion is other than zero can be treated as an incubative period determining the time needed for the structural transition to be prepared. This time is a constant for a particular material and is independent of the loading velocity [17, 18]. It is the difference in the incubative period of mesostructure formation that is responsible for the difference in velocities of the steady-state plastic fronts for the materials of the first and second types.

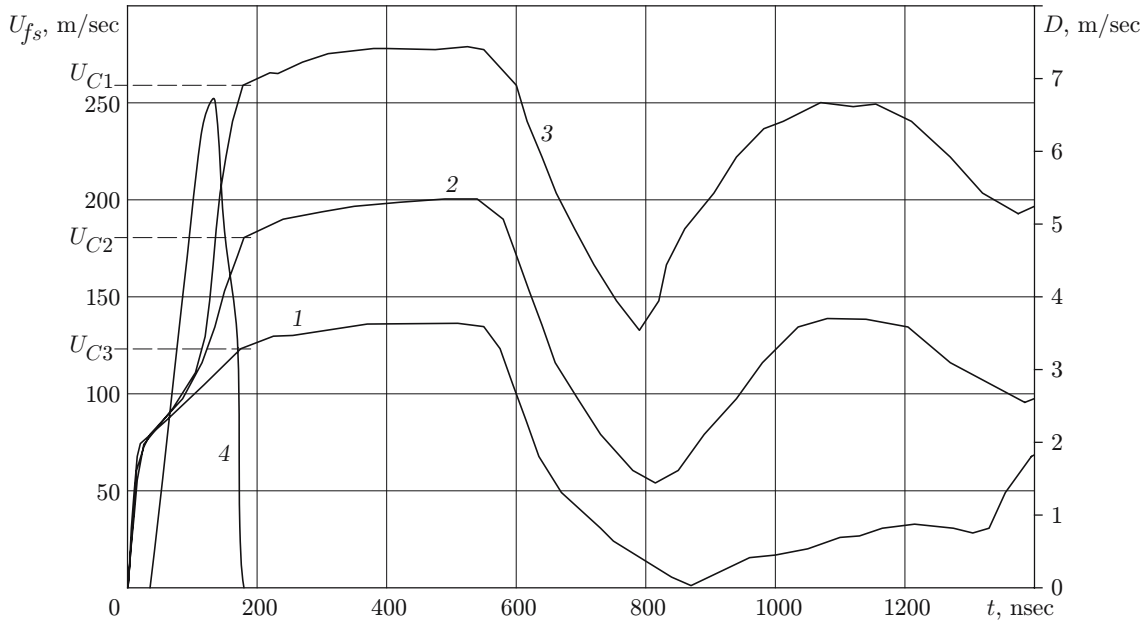

Fig. 3. Velocity of the free surface (1–3) and root-mean-square deviation of velocity (4) versus time ($\delta = 1.6$ μm): $U_{\text{imp}} = 136.2$ (1), 200 (2), and 280.3 m/sec (3).

At the moment, real-time visual registration of the structural transition during high-velocity deformation of solids does not seem possible because the time of the processes under study is too short. Nevertheless, there is some indirect evidence of the existence of structural transitions of this kind: 1) the presence of the mass velocity dispersion at mesolevel 2 (see [1]) registered in the case of dynamic deformation of beryllium and Armco iron [19] and also tantalum [20]; 2) material fragmentation observed in the spall zone with an exceeded threshold stress of the structural transition in high-tensile steels and other structural materials [21, 22]. There is no such fragmentation if the stress on the plastic front is smaller than a certain value at which a mass velocity defect appears on the compression pulse plateau.

Under conditions of quasi-static deformation of a solid, where the system is close to thermodynamic equilibrium, mesostructures have the meaning of dissipative structures known in synergetics [23]. In the case of dynamic deformation of a solid, mesostructures emerging on the plastic front have the meaning of dynamic structures. In a turbulent fluid, these structures, which are commonly called large-scale oscillations, are reversible formations [24]. Dynamic structures arising under shock deformation of a solid can also be reversible if the stress on the plastic front does not reach the critical value. One criterion determining the conditions of irreversibility of these structures was obtained in [2].

Thus, by comparing the dependences of mass velocity on time for two structures of the material, we could find the difference in their response to shock loading. In the coarse-grain material, generation of the structure of mesolevel 2 is caused by separation of grains into blocks, which requires a certain energy to be spent. For the fine-grain material, there are no such losses, because this material already has the structure of mesolevel 2 in the initial state. Formation of a new structural level in the fine-grain material, which is not related to the original structure, is actually material fragmentation. Therefore, subsequent unloading on the rear front of the pulse and extension in the spall zone occur in a partly weakened material, which decreases the spall strength, as compared to the spall strength of the fine-grain material.

Figure 2 shows the threshold velocity of the beginning of the structural transition U_C as a function of the impact velocity U_{imp} for the aluminum alloys of the first and second types. In the entire range of impact velocities, these dependences are seen to be in good agreement. This testifies that the threshold velocity of the structural transition for the 1420 aluminum alloy is independent of its state (coarse grains or fine grains). As the slope of the plastic front for the materials of both types changes at an identical mass velocity for one value of the impact velocity, the difference in the response of the examined materials to shock compression is manifested only in the

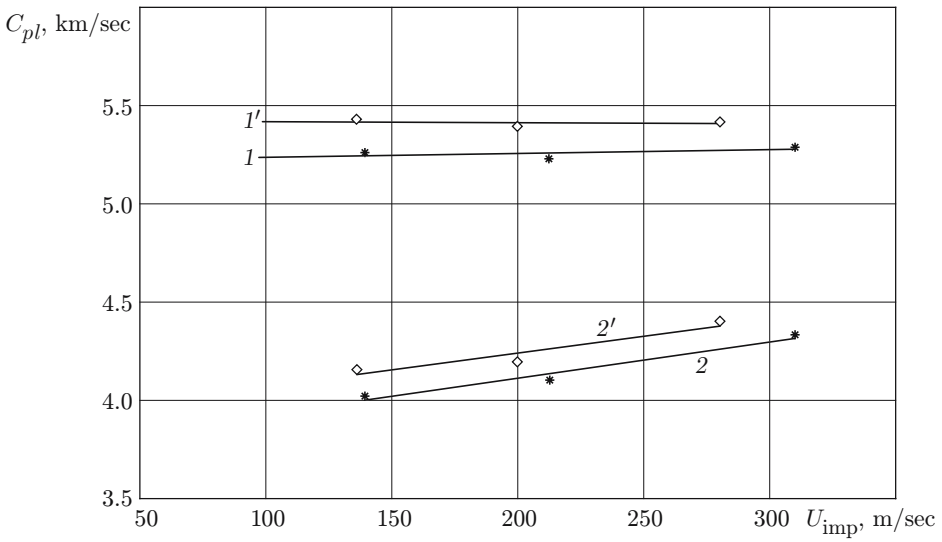

Fig. 4. Velocities of the first (1 and 1′) and second (2 and 2′) plastic fronts versus the impact velocity: $\delta = 24$ (1 and 2) and 1.6 μm (1′ and 2′).

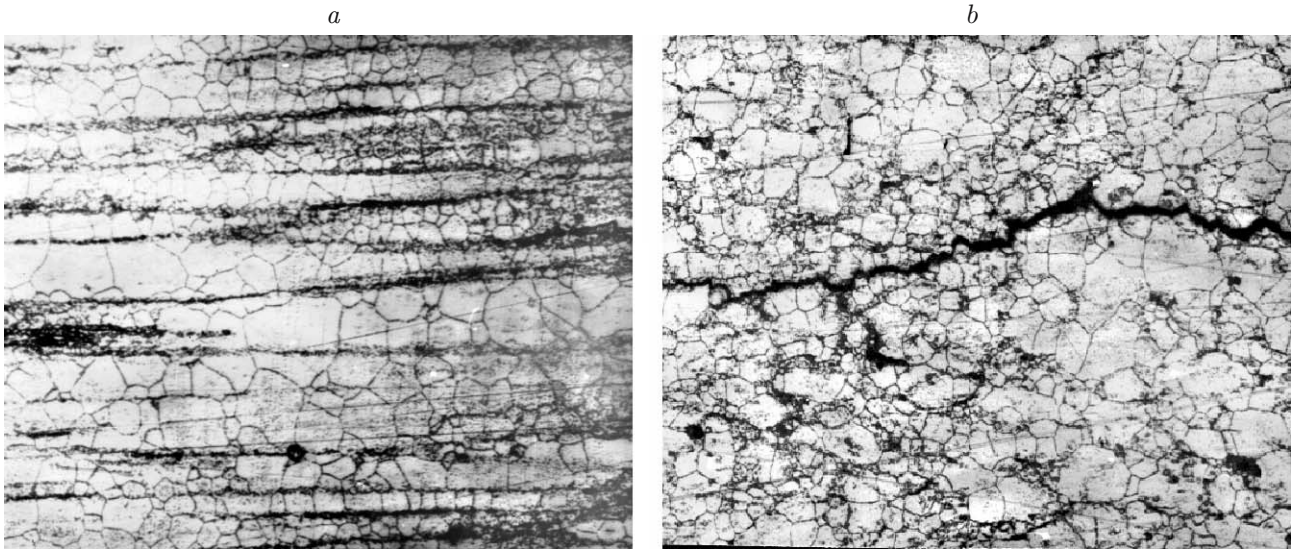

Fig. 5. Structure of the coarse-grain 1420 aluminum alloy (×200): $U_{\text{imp}} = 97.2$ (a) and 139.1 m/sec (b).

difference in the mass velocity defect on the gently sloping part of the front (segment $CDEF$ in Fig. 1). The increase in velocity on the DE segment may be considered as the second plastic front propagating in the material with a changed structure, i.e., after the structural phase transition. In this case, instead of a two-wave structure of the mass velocity profile, like in any phase transition initiated by shock loading, we have a three-wave structure consisting of an elastic precursor, first plastic front, and second plastic front.

Figure 4 shows the velocities of propagation of the first and second plastic fronts as functions of the impact velocity for the materials of both types. The values of velocities were determined on the basis of the delay of the front with respect to the elastic precursor on the velocity profile of the free surface; the reference point for the second front was the middle of this time period [25]. In the examined range of impact velocities, the velocity of the first plastic front is seen to remain unchanged, though it is slightly higher for the fine-grain aluminum alloy than for the coarse-grain material, as was noted above. The constant velocity means that the first plastic front is stationary. The velocity of the second plastic front is approximately 1.3 times lower than the velocity of the first plastic front and increases with increasing impact velocity, in contrast to the velocity of the first plastic front.

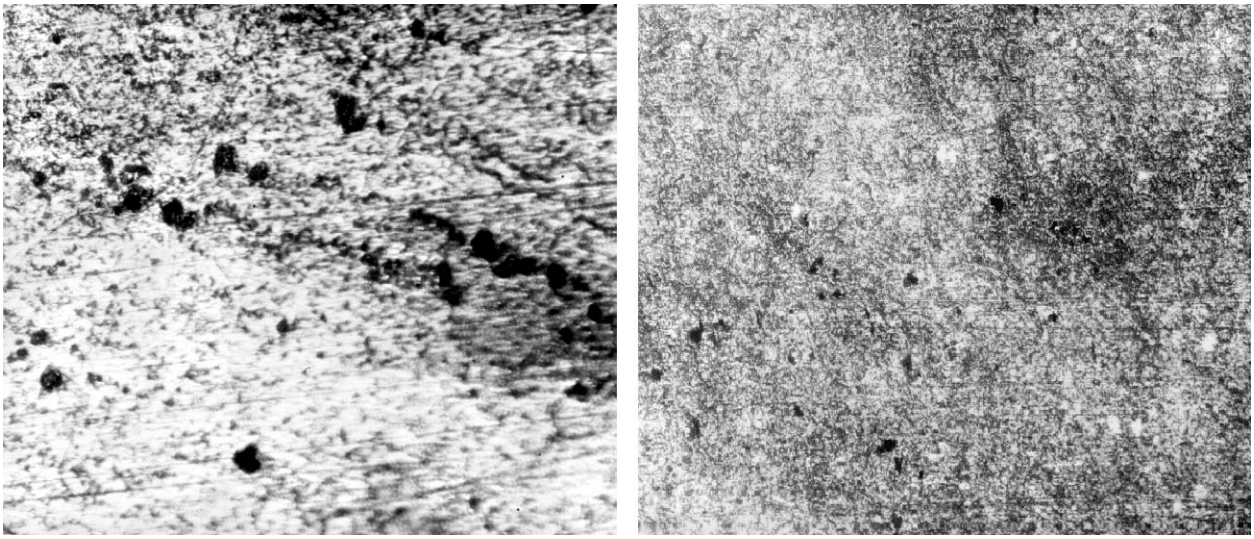

Fig. 6. Structure of the fine-grain 1420 aluminum alloy (×200): $U_{\text{imp}} = 98.8$ (a) and 124 m/sec (b).

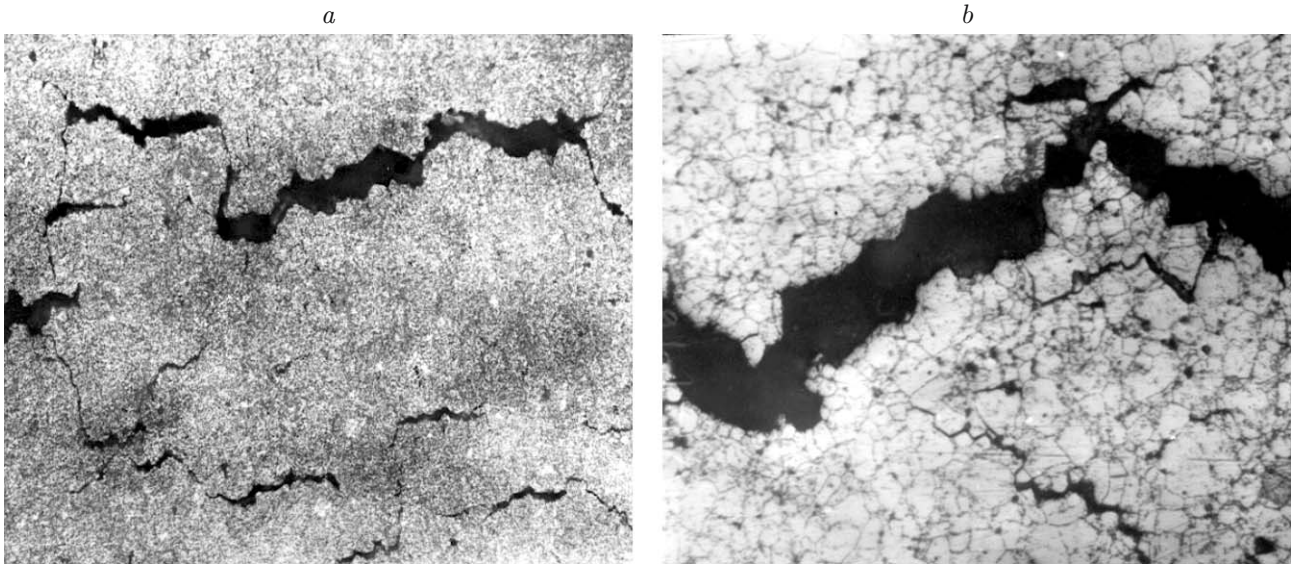

Fig. 7. System of cracks in the spall region (×200): (a) $\delta = 1.6$ μm and $U_{\text{imp}} = 200$ m/sec; (b) $\delta = 24$ μm and $U_{\text{imp}} = 212.5$ m/sec.

The method of the description of hierarchic "addition" of structures of different scales, which is similar to the method considered in the present paper, implies that there are changes in the spectrum of defects participating in high-velocity plastic deformation [26]. Such a method does not contradict the above-described concepts of the change in the material structure with the change in loading stresses.

3. Microstructural Studies. After the shock tests, all samples were cut in one plane along the wave-propagation direction and were studied by methods of optical and scanning electron microscopy. In the initial state, the 1420 aluminum–lithium alloy was an oversaturated solid solution with respect to magnesium and lithium with fine particles of the δ' phase (Al_3Li) and S phase (Al_2LiMg). The mean macrohardness of the material in the initial state was HB = 97.4 kg/mm^2. Shock loading does not affect the macrohardness in the entire range of loading velocities. In the range of velocities between 139.1 and 212.5 m/sec, however, both the grain size and the

shape and locations of particles of the S phase are changed. The mean grain size decreases from 24 to 18 μm. The S phase has the shape of long "linear" structures crossing the grains in the initial state and outside the range of 139.1 to 212.5 m/sec (Fig. 5a), but the S-phase particles in the indicated range of velocities acquire a circular shape and are mainly located on the grain boundaries (Fig. 5b). Despite these changes in the material structure, no significant changes in the spall strength of the coarse-grain material are observed in this range of impact velocities. The absence of the influence of S-phase redistribution owing to shock loading on the spall strength of this alloy indicates that spall fracture is caused by processes proceeding at a larger-scale mesolevel 2 (the particle size in the S phase corresponds to mesolevel 1).

After equal-channel angular pressing, the grains acquire a uniaxial shape with a mean grain size $\delta = 1.6$ μm. Shock loading in the range of impact velocities of 98.7 to 280.3 m/sec increases the hardness to HB = 124 kg/mm^2, which is 36.6 kg/mm^2 greater than that in the coarse-grain material. Shock loading of the material with the smaller grain size leads to structural changes approximately in the same range of impact velocities equal to 124 to 200 m/sec. The S phase becomes distributed more uniformly, and its particles become smaller (Fig. 6). No significant changes in the spall strength of the material in this range of impact velocities are observed.

For identical impact velocities, the system of cracks in the spall zone of the coarse-grain alloy is more developed than that in the alloy with a grain size $\delta = 1.6$ μm (Fig. 7).

Conclusions. Through comparisons of the dynamic response of the 1420 aluminum alloy in two structural state differing by the grain size, it is demonstrated that there is a threshold strain rate under uniaxial strain conditions, which is responsible for origination of a new structural level in a crystalline material. This level can be considered as a structural phase transition. The emergence of a large-scale dynamic structure evidences fragmentation of the granular structure, which reduces the spall strength.

REFERENCES

1. V. E. Panin (ed.), *Physical Mesomechanics and Computer-Aided Design of Materials* [in Russian], Nauka, Novosibirsk (1995).
2. Yu. I. Meshcheryakov, "On evolutionary and catastrophic regimes of energy transfer in dynamically loaded media," *Dokl. Ross. Akad. Nauk*, No. 6, 765–768 (2005).
3. T. A. Khantuleva and Yu. I. Meshcheryakov, "Kinetics and nonlocal hydrodynamics of mesostructure formation in dynamically deformed media," *Fiz. Mezomekh.*, **2**, No. 5, 5–17 (1999).
4. Yu. I. Mescheryakov, "Meso-macro energy exchange in shock deformed and fractured solids," in: Yu. Ya. Horie, L. Davison, and N. N. Thadhani (eds.), *High-Pressure Shock Compression of Solids VI*, Springer-Verlag, New York (2002), pp. 169–213.
5. R. Z. Valiev and I. V. Aleksandrov, *Nanostructural Materials Obtained Under Intense Plastic Strains* [in Russian], Logos, Moscow (2000).
6. Yu. I. Mescheryakov and A. K. Divakov, "Multiscale kinetics of microstructure and strain-rate dependence of materials," *Dynamic Mater. J.*, **1**, No. 4, 271–287 (1994).
7. G. I. Kanel', S. V. Razorenov, A. V. Utkin, and V. E. Fortov, *Shock-Wave Phenomena in Condensed Media* [in Russian], Yanus, Moscow (1996).
8. L. M. Barker, C. D. Lundergun, and W. Herrmann, "Dynamic response of aluminium," *J. Appl. Phys.*, **35**, No. 4, 1203–1212 (1964).
9. J. W. Taylor and M. H. Rice, "Elastic-plastic profiles in iron," *J. Appl. Phys.*, **34**, 365–368 (1963).
10. D. E. Grady, "Metallurgical applications of shock-wave phenomena," in: L. E. Murr, K. P. Staudhammer, and M. A. Meyers (eds.), *Metallurgical Applications of Shock-Wave and High-Strain-Rate Phenomena*, Marcell Dekker, New York (1986), pp. 763–780.
11. G. I. Kanel, S. V. Rasorenov, and V. E. Fortov, *Shock-Wave Phenomena and the Properties of Condensed Matter*, Springer-Verlag, New York (2004).
12. J. J. Gilman, "Mechanical states of solids," in: M. D. Furnish, N. N. Thadhani, and Y. Horie (eds.), *Shock Compression of Condensed Matter-2001*, Amer. Inst. of Phys., Melville–New York (2002), pp. 36–41.
13. P. V. Makarov, "Loaded material as a nonlinear dynamic system. Problems of modeling," *Fiz. Mezomekh.*, **8**, No. 6, 39–56 (2005).

14. L. M. Barker and R. E. Hollenbach, "Shock wave study of the $\alpha \leftrightarrow \varepsilon$ phase transition in iron," *J. Appl. Phys.*, **45**, No. 11, 4872–4887 (1974).
15. D. E. Duvall, "Maxwell-like relations in condensed matter. Decay of shock waves," *Irish J. Phys. Tech.*, **7**, 57–69 (1978).
16. É. L. Aéro, "Microscale deformations in two-dimensional lattice structural transitions under critical shear," *Fiz. Tverd. Tela*, **42**, No. 6, 1147–1153 (2000).
17. Yu. V. Petrov and N. F. Morozov, "On modeling of fracture of brittle solids," *J. Appl. Mech.*, **61**, 710–712 (1994).
18. A. A. Grudskov and Yu. V. Petrov, "Temperature–time correlation during high-velocity deformation of metals," *Dokl. Ross. Akad. Nauk*, **364**, No. 6, 766–768 (1999).
19. Yu. I. Mescheryakov, A. K. Divakov, Yu. A. Petrov, and C. F. Cline, "On the dynamic plasticity and strength of crystalline beryllium," *Int. J. Impact Eng.*, **30**, 17–29 (2004).
20. L. C. Chhabildas, W. M. Trott, W. D. Reinhart, and G. A. Mann, "Incipient spall studies in tantalum. Microstructural effects," in: M. D. Furnish, N. N. Thadhani, Y. Horie (eds.), *Shock Compression of Condensed Matter-2001*, Amer. Inst. of Phys., Melville–New York (2002), pp. 483–486.
21. Yu. I. Meshcheryakov and A. K. Divakov, "Effect of processes at the compression pulse front on spalling strength of a material and resistance to high-velocity penetration," *J. Appl. Mech. Tech. Phys.*, **44**, No. 6, 770–778 (2003).
22. Yu. I. Mescheryakov, A. K. Divakov, Yu. A. Petrov, et al., "Comparative analysis of uniaxial strain shock tests and Taylor tests for armor and maraging steels," *High Pressure Res.*, **24**, 263–274 (2004).
23. H. Haken, *Advanced Synergetics. Instability Hierarchies of Self-Organizing Systems and Devices*, Springer, Heidelberg (1983).
24. L. D. Landau and E. M. Lifshits, *Course of Theoretical Physics*, Vol. 6: *Fluid Mechanics*, Pergamon Press, Oxford-Elmsford, New York (1987).
25. L. M. Barker, "α-Phase Hugoniot of iron," *J. Appl. Phys.*, **46**, No. 6, 2544–2547 (1975).
26. G. I. Kanel', S. V. Razorenov, and V. E. Fortov, "Submicrosecond strength of materials," *Izv. Ross. Akad. Nauk, Mekh. Tverd. Tela*, No. 4, 86–111 (2005).